

Improving of ultracold neutron traps coated with liquid helium using capillarity and electric field

Pavel D. Grigoriev,^{1,2,*} Arseniy V. Sadovnikov,^{3,4} Vladislav D. Kochev,² and Alexander M. Dyugaev¹

¹*L. D. Landau Institute for Theoretical Physics, 142432, Chernogolovka, Russia*

²*National University of Science and Technology "MISiS", 119049, Moscow, Russia*

³*Lomonosov Moscow State University, 119991, Russia*

⁴*I.M. Sechenov First Moscow State Medical University, 119991, Russia*

To increase the storage time of ultracold neutrons (UCN) inside the material traps it is promising to cover the trap walls by liquid ^4He , the material which does not absorb neutrons at all. A rough side wall of UCN trap holds the required amount of ^4He by the capillary effects, but the edges of wall roughness remain insufficiently coated. Here we propose to apply an electric voltage to these rough side walls of UCN traps to increase the thickness of liquid He on the wall edges and to cover the entire wall surface by sufficiently thick helium films. This completely protects UCN from being absorbed inside the trap walls. We estimate the required electric field and voltage for several possible designs of UCN traps. This improvement may give rise to a new generation of ultracold neutron traps with very long storage time. We also estimate the influence of this electric field on the dispersion of ripplons – the quanta surface waves, which give the main contribution to the inelastic UCN scattering at low temperature.

I. INTRODUCTION

The precise measurements of neutron lifetime τ_n are important for elementary particle physics, astrophysics and cosmology (see [1–5] for reviews). The Big-Bang nucleosynthesis and chemical element formation depends on τ_n . In combination with spin-electron asymmetry measured in polarized-neutron decay experiments [6–8] the τ_n measurements give both vector and axial coupling constants of weak interaction in hadronic current between nucleons, which differs from the quark current due to a renormalization by strong interaction. The search for a non-zero electric dipole moment (EDM) of neutrons [9–11] impose the limits on CP violation. The resonant transitions between discrete quantum energy levels of neutrons in the earth gravitational field [12, 13] probe the gravitational field on a micron length scale and impose constraints on dark matter.

The ultracold neutrons (UCN) with energy lower than the neutron optical potential of typical materials, i.e. $\lesssim 300$ neV, are widely employed in neutron experiments [6, 8, 10–21]. These UCN can be trapped for many minutes in specially designed "neutron bottles" [17–21], where the earth gravitational field 100 neV per meter plays an important role in UCN storage and manipulation [14–21]. The Fomblin grease is currently used to cover the UCN trap walls [17–23] in the bottle UCN experiments and allows reaching the highest accuracy of neutron lifetime measurements: $\tau_n = 881.5 \pm 0.7(\text{stat}) \pm 0.6(\text{syst})$ s [20]. Because of the neutron magnetic moment of 60 neV/T, magneto-gravitational trapping of UCN is feasible and promising too [24–28], giving a comparable claimed accuracy. However, the non-uniformity of magnetic field produces considerable losses of spin-polarized UCN in such magnetic traps, and an accurate estimate of these losses to account them for is a difficult problem. Therefore, in spite of high claimed precision of magnetic-trap τ_n measurements, the corresponding values [27] $\tau_n \approx 878.3 \pm 1.6(\text{stat}) \pm 1.0(\text{syst})$ s or [28] $\tau_n \approx$

$877.7 \pm 0.7(\text{stat})_{-0.2}^{+0.4}(\text{syst})$ s are about 4 s smaller than in the material-bottle UCN experiments.

The main alternative to using UCN in neutron lifetime measurements is the cold neutron beam, giving $\tau_n = 887.7 \pm 1.2(\text{stat}) \pm 1.9(\text{syst})$ s [29–31]. The discrepancy between τ_n measured by beam and UCN material- or magnetic-trap methods is beyond the estimated errors. This "neutron lifetime puzzle" is a subject of extensive discussion till now [31–34]. Presumably, it is due to systematic errors in beam experiments [33], but unconsidered UCN losses in bottle τ_n measurements are not excluded yet. As has been shown by analyzing the neutron β -decay asymmetry [35], it is unlikely that this discrepancy is caused by other new physics like additional neutron decay channels or dark matter [31, 32]. Hence, reducing the UCN losses in material traps is crucial for various neutron experiments.

The precision of current neutron lifetime measurements using UCN traps, both material and magnetic, is limited by the accuracy of estimating of neutron escape rate from the traps, which is the main source of systematic errors [14–16, 20, 21, 36]. At present, material UCN traps coated with Fomblin grease provided the highest accuracy of τ_n measurements. Any collision of a neutron with trap wall leads to $\sim 10^{-5}$ probability of neutron absorption by the wall material [4, 14–16]. The neutron lifetime τ_n is estimated by extrapolation of the measured lifetime τ_1 of neutrons stored in the trap to the zero neutron losses by a careful variation of the bottle geometry and/or temperature, so that the loss contribution from trap walls can be accounted for. The extrapolation interval is rather large, usually, $\tau_n - \tau_1 \gtrsim 30$ s, which limits the precision of τ_n measurements, because estimating the systematic error with accuracy better than 5% is a very hard problem. The surface-to-volume ratio in material traps and the UCN losses on trap walls can be reduced by increasing the trap size. Note that the UCN material traps covered by Fomblin oil must be kept at a low temperature $T < 90$ K to reduce the inelastic neutron scattering. In most precise recent τ_n measurements [20] the extrapolation interval $\tau_n - \tau_1$ was reduced to only 20 seconds by increasing the size of high-vacuum UCN material trap to 2 m, making the dimensions of external vacuum vessel

* grigorev@itp.ac.ru

4.2 m. However, a further size increase of UCN traps seems technically problematic and not very useful, because main neutron losses come from their collisions with trap bottom rather than with its side walls.

A possible qualitative step to further reduce the neutron escape rate from UCN traps is to cover the trap walls by liquid ^4He , the only material that does not absorb neutrons [37–39]. However, ^4He provides a very small optical potential barrier $V_0^{\text{He}} = 18.5$ neV for the neutrons, which is much smaller than the barrier height $V_0^{\text{F}} \approx 106$ neV of Fomblin oil. Only UCN with kinetic energy $E < V_0^{\text{He}}$ can be effectively stored in such a trap. The corresponding maximum height of UCN $h_{\text{max}} = V_0^{\text{He}}/m_n g \approx 18$ cm, where $m_n = 1.675 \times 10^{-24}$ g is the neutron mass. The UCN phase volume and their density in the He trap is reduced by the factor $(V_0^{\text{F}}/V_0^{\text{He}})^{3/2} \approx 13.7$ as compared to the Fomblin coating. This raises the statistical errors. However, the UCN density increases as technology develops [40, 41], and this reduction of neutron density may become less important than the advantage from a decrease of UCN loss rate.

The second problem with the liquid ^4He coating of UCN trap walls is a very low temperature $T < 0.5$ K. At higher temperature ^4He vapor inelastically scatters UCN, giving them energy $\sim k_B T \gg V_0^{\text{He}}$. At $T < 0.5$ K the concentration of ^4He vapor $n_V \propto \exp(-7.17/T [\text{K}])$ is negligibly small. Another source of inelastic UCN scattering are ripplons, the thermally activated quanta of surface waves. They lead to a linear temperature dependence of scattering rate [42], surviving even at ultralow temperature. However, the strength of neutron-riplon interaction is rather small [42], which makes feasible the UCN storage in He-covered traps. Moreover, the linear temperature dependence of UCN losses due to their scattering by ripplons is very convenient for taking into account this systematic error.

The third problem with liquid ^4He is too thin helium film covering the side walls of the trap. ^4He is superfluid below $T_\lambda = 2.17$ K and covers not only the floor but also the walls and the ceiling of the trap because of the van-der-Waals attraction. On flat vertical walls few centimeters above the He level, the thickness of helium film is expected to be only $d_{\text{He}}^{\text{min}} \approx 10 \text{ nm} < \kappa_{0\text{He}}^{-1}$, while the neutron penetration depth into the liquid helium is $\kappa_{0\text{He}}^{-1} = \hbar/\sqrt{2m_n V_0^{\text{He}}} \approx 33.3 \text{ nm} > d_{\text{He}}$. Hence, the tunneling exponent

$$\psi(0)/\psi(d_{\text{He}}) \sim \exp(-\kappa_{0\text{He}} d_{\text{He}}), \quad (1)$$

of the neutron wave function ψ inside He is not sufficient to strongly reduce the neutron losses on the trap walls. A more accurate calculation of the neutron wave function near a solid wall covered with liquid helium [43] increases the estimate of $\psi(0)$ by $\sim 30\%$ as compared to Eq. (1) for relevant UCN kinetic energy $E < 0.8V_0^{\text{He}}$, making the problem of too thin ^4He film even more serious. The required thickness of helium film for a good protection of UCN is $d \leq d_{\text{He}}^* = 100 \text{ nm}$ [43]. An idea [38] of using a rotating He vessel for UCN storage to increase He thickness on side walls has a drawback that the rotating liquid generates additional bulk and surface excitations, leading to inelastic neutron scattering. Therefore,

one needs a time-independent covering of the trap walls by liquid ^4He . A possible solution of this problem, proposed recently [43, 44], is based on using a rough surface of trap side walls. This rough surface holds liquid helium of sufficient thickness by the capillary effect, if the wall roughness has much smaller period l_R than the ^4He capillary length $a_{\text{He}} = \sqrt{\sigma_{\text{He}}/g\rho_{\text{He}}} = 0.5 \text{ mm}$, where $\sigma_{\text{He}} = 0.354 \text{ dyn/cm}$ is the surface tension coefficient of liquid ^4He , $g = 980 \text{ cm/s}^2$ is the free fall acceleration, and the liquid ^4He density $\rho_{\text{He}} \approx 0.145 \text{ g/cm}^3$. The calculations showed [43, 44] that one needs even the smaller period of wall roughness $l_R \lesssim 4a_{\text{He}}^2/h$ to hold superfluid ^4He on the height h above the helium level.

In Ref. [44] it was argued that a simple triangular wall roughness of period $l_R \lesssim 5 \mu\text{m}$, as in the mass-produced diffraction gratings [45], is better than rectangular roughness to hold a shielding helium film in UCN traps. The diffraction gratings with the period $l_R \approx 4 \mu\text{m}$ and depth $h_R \approx 0.2 \mu\text{m}$ are already actively used for the scattering of UCNs [46, 47]. However, the thickness of He film on sharp peaks of this triangular roughness remains less than $\kappa_{0\text{He}}^{-1}$, which leaves $\lesssim 5\%$ of wall surface insufficiently coated. In this paper we propose to use an electrostatic potential to increase the efficiency of such helium-covered UCN traps and to coat the remaining unshielded surface area. This may completely eliminate the UCN losses from the absorption inside the trap walls and start a new generation of ultracold neutron traps with very long storage time.

II. ENERGY FUNCTIONAL OF LIQUID HELIUM AND REQUIRED FIELD STRENGTH

To describe the profile of the helium film on the rough surface, it is necessary to minimize the energy functional of this film

$$E_{\text{tot}} = V_g + E_s + V_w + V_e. \quad (2)$$

This functional (2) differs from that considered in Refs. [43, 44] by the new term V_e , which comes from the polarization energy of helium in a non-uniform electric field, as described below. The first three terms in Eq. (2) are the same as in Refs. [43, 44]. V_g is the gravity term given by the expression

$$V_g = \rho_{\text{He}} g \int z d_{\text{He}}(\mathbf{r}_{\parallel}) d^2 \mathbf{r}_{\parallel}, \quad (3)$$

where $\mathbf{r}_{\parallel} = \{x, z\}$ is the two-dimensional vector of the horizontal, x , and vertical, z , coordinates on the wall,

$$d_{\text{He}}(\mathbf{r}_{\parallel}) = \xi(\mathbf{r}_{\parallel}) - \xi_w(\mathbf{r}_w) \quad (4)$$

is the thickness of the helium film. The functions $\xi(\mathbf{r}_{\parallel})$ and $\xi_w(\mathbf{r}_{\parallel})$ describe the profiles of the He surface and of the solid trap wall.

The second term E_s in Eq. (2) describes the surface tension energy and is given by the formula

$$E_s = \sigma_{\text{He}} \int \left(\sqrt{1 + [\nabla \xi(\mathbf{r}_{\parallel})]^2} - 1 \right) d^2 \mathbf{r}_{\parallel}. \quad (5)$$

Here we subtracted the constant term of a flat surface $E_{s0} = \sigma_{\text{He}} \int d^2 \mathbf{r}_{\parallel}$.

The third van der Waals term V_W in Eq. (2) describes the attraction of helium to the wall material. It is significant only at small distance and leads to coating of the entire wall surface by a superfluid helium film thicker than $d_{\text{He}}^{\text{min}} \approx 10$ nm. As shown in Refs. [43, 44], the capillary effects compensate the gravity term and hold much thicker helium film on the height h above helium level if the characteristic length scale of the wall roughness does not exceed $l_R^{\text{max}} = 4a_{\text{He}}^2/h$. For the wall roughness of the shape of a triangular grid, as proposed in Ref. [44], l_R^{max} gives its maximal period.

The electric energy term E_e in Eq. (2), describing the polarization energy of helium in a non-uniform electric field, is

$$E_e = -\frac{\varepsilon_{\text{He}} - 1}{4\pi} \int E^2(\mathbf{r}) d^3 \mathbf{r}, \quad (6)$$

where the integral is taken over the volume occupied by liquid He, and $\varepsilon_{\text{He}} = 1.054$ is the dielectric constant of ^4He . On the trap side wall Eq. (6) rewrites as

$$E_e = -\frac{\varepsilon_{\text{He}} - 1}{4\pi} \int E^2(\mathbf{r}_{\parallel}, d_{\text{He}}) d_{\text{He}}(\mathbf{r}_{\parallel}) d^2 \mathbf{r}_{\parallel}. \quad (7)$$

This term is new as compared to Refs. [43, 44].

The surface profile of superfluid ^4He corresponds to the constant energy $E_{\text{tot}} = E_0 = \text{const}$ in Eq. (2) of a tiny helium volume. This constant energy is the same, as for liquid ^4He on the surface above the bottom of UCN trap. Eqs. (2)-(6) assume liquid helium to be incompressible, which is a rather good approximation. To find the ^4He surface profile on the side wall one needs to know the spatial distribution of the absolute value of electric field strength $E^2(\mathbf{r})$.

The capillary effects do not help to cover the wall edges by a sufficiently thick helium film. Eqs. (2),(3) and (7) allow to estimate the required electric field strength $E_*(h)$ at the surface of liquid helium on the side wall at height h to hold the helium film even without the capillary effects. The electric term (7) compensates the gravity term (3) if $V_g + E_e < 0$, which gives the electric field strength

$$E \geq E_* = \sqrt{\rho_{\text{He}} g h \cdot 4\pi / (\varepsilon_{\text{He}} - 1)}. \quad (8)$$

For $h = h_{\text{max}} = 18$ cm this gives a target electric field $E_* \approx 230$ kV/cm. Such a strong electric field appears because of a weak ^4He polarization, $\varepsilon_{\text{He}} - 1 = 0.054 \ll 1$. Nevertheless, it is still much smaller than the field of dielectric breakdown $E_{\text{max}} > 1$ MV/cm of ^4He [48]. Therefore, it is theoretically achievable.

Fortunately, one does not need to apply such a strong field E_* at the whole side-wall surface but only near the edges of its roughness. Near these edges the electric field can be easily increased if the rough wall itself serves as an electrode. Below we consider this in more detail for the triangular wall roughness and show, that we need an external electric field E_0 several times weaker than E_* .

III. ELECTRIC FIELD STRENGTH AND HELIUM FILM THICKNESS NEAR A TRIANGULAR EDGE

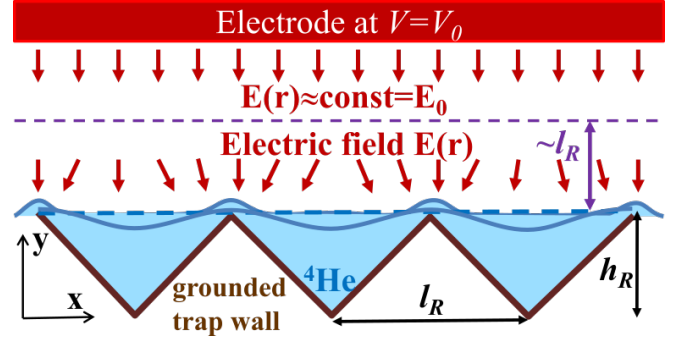


Figure 1. Triangular roughness (brown polyline) of solid UCN trap wall coated with liquid helium with periodically modulated surface (blue solid line). The applied electric field is the strongest near the wall edges, which attracts ^4He to these edges and coat them with a helium film of sufficient thickness.

We consider a grounded metallic rough trap wall with voltage $V = 0$ covered with ^4He . Another electrode at voltage V_0 is separated at some characteristic distance L (see Fig. 1). The electric potential $V(\mathbf{r})$ raises from $V = 0$ at the wall surface to V_0 at this electrode. Possible trap designs are discussed in Sec. V.

The side-wall material can be beryllium, copper, or any other metal with a weak neutron absorption and a rough surface to hold ^4He film. We consider a one-dimensional triangular roughness with period $l_R \sim 10$ μm and depth $h_R \sim 1$ μm , as proposed in Ref. [44] and illustrated in Fig. 1. According to Ref. [44], ^4He film covering this wall is thick enough to protect UCN from the absorption everywhere except the sharp triangular edges of the wall. Fortunately, near these edges the electric field strength $E(\mathbf{r})$ is much higher than the electric field $E_0 \sim V_0/L$ far from this edge, so that the last electric term in Eqs. (6) or (7) is large enough to hold a sufficiently thick helium film. To estimate the ^4He film thickness near this corner we first need to calculate the strength distribution of electric field. Since the ^4He dielectric constant $\varepsilon_{\text{He}} = 1.054$ is close to unity, we may disregard the back influence of ^4He on electric field, performing the calculations for metal-vacuum interface.

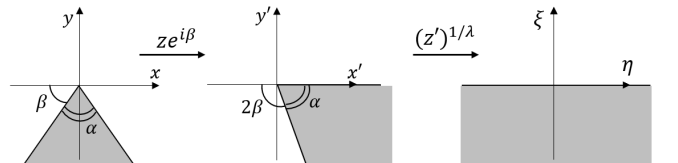


Figure 2. Conformal mapping of infinitely long edge of angle $\alpha = \pi - 2\beta$, used to find the solution of Laplace equation for electrostatic potential.

To estimate the electric field near an infinitely long edge of angle $\alpha = \pi - 2\beta$, $0 < \beta < \pi/2$ (see Fig. 2), we use

the standard method of conformal mapping of dimensionless complex coordinate $z_c \equiv (x + iy)/l = r \exp(i\phi)/l$ to $\zeta \equiv u + iv = \rho \exp(i\theta)$ [49]:

$$\zeta = \left(z_c e^{i\beta} \right)^{1/\lambda} = r^{1/\lambda} \exp[i(\phi + \beta)/\lambda], \quad (9)$$

where $\lambda = 1 + 2\beta/\pi$. This mapping transforms the angle to a line and allows an easy calculation of the electric potential as

$$V(\zeta(z)) = \Delta V_0 \text{Im} \zeta = \Delta V_0 r^{1/\lambda} \sin[(\phi + \beta)/\lambda], \quad (10)$$

where ΔV_0 is the potential raise per the normalization distance l . The electric field strength near the edge is

$$|E| = E_0 \left| \frac{d\zeta}{dz_c} \right| = \frac{E_0}{\lambda} |z_c|^{1/\lambda - 1}, \quad (11)$$

where $E_0 = \Delta V_0/l$ is the electric field far from the edge. In our case of periodic triangular wall roughness, shown in Fig. 1, the characteristic length scale $l = l_R \sim 10 \mu\text{m}$, because at a distance $r \gg l_R$ from the edge the electric field does not have singularity and is almost uniform as near a flat wall. The electric field squared at $r \ll l_R$

$$E^2(r) = \frac{E_0^2}{\lambda^2} \left(\frac{l_R}{r} \right)^{4\beta/(\pi+2\beta)}. \quad (12)$$

At a distance r from the edge the electric field $E(r)$ is larger than the average electric field $E_0 \approx V_0/L$ by a factor of

$$\gamma = E(r)/E_0 = (l_R/r)^{2\beta/(\pi+2\beta)} / (1 + 2\beta/\pi). \quad (13)$$

We are interested to coat the edge of wall roughness with the ^4He film of thickness $d_{\text{He}}^* \approx 100 \text{ nm}$. At $r = d_{\text{He}}^* = 100 \text{ nm}$, $l_R = 10 \mu\text{m}$ and $\beta = \pi/3$ this parameter $\gamma = E(d_{\text{He}}^*)/E_0 \approx 3.8$, while at $\beta = \pi/4$ we obtain $\gamma = E(d_{\text{He}}^*)/E_0 \approx 3.1$.

In Eqs. (12)-(13) $E(r) \rightarrow \infty$ at $r = 0$ because we took an infinitely sharp edge. The actual curvature radius at the edge R_c is finite, and Eqs. (11)-(13) are valid at $r \gg R_c$. Hence, we may use Eqs. (11)-(13) at the ^4He free surface if the curvature radius is much smaller than the depth of ^4He film at the edge, $R_c \ll d_{\text{He}}^*$. In the derivation of Eqs. (10)-(13) we considered a single edge. This imposes another restriction on using Eqs. (11),(12): $r \ll l_R$. Thus, Eqs. (10)-(12) hold if

$$R_c \ll r \approx d_{\text{He}}^* \approx 100 \text{ nm} \ll l_R \sim 10 \mu\text{m}. \quad (14)$$

The electric-field distribution $E(r)$ near a periodic boundary, such as a rectangular diffraction grating, can be studied using the Fourier series and Rogowski's or Roth's methods (see ch. 5 of [49]), but it is much more complicated and gives a less visual result.

In our physical problem the condition (14) is satisfied, but there is another source of possible quantitative error – the cut-off choice $l = l_R$. This choice is only qualitatively correct, i.e. up to a factor ~ 1 . To analyze the possible error we performed the numerical calculation of the electric field distribution by solving the Laplace equation for the electrostatic potential $V(r)$ using the method of finite elements. The boundary conditions

are taken as $V = 0$ at the rough trap wall of the periodic triangular shape, as shown in Fig. 1, and $V = V_0$ at the flat electrode parallel to this wall. Thus, the numerical problem is 2D. The result of this calculation for the electric field distribution is given in Fig. 3a, and the comparison of calculated parameter $\gamma(r) = E(r)/E_0$ with Eq. (13) is shown in Fig. 3b for several edge angles $\alpha = \pi - 2\beta$.

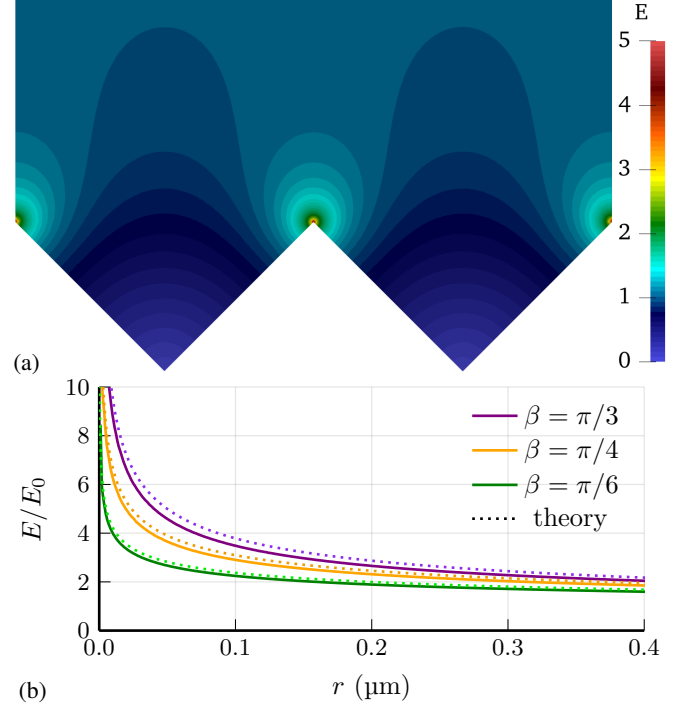


Figure 3. Numerical results for the electric field distribution $E(r)$ near a equipotential wall having the shape of a triangular grid, i.e. a triangular groove periodically repeated along the wall. (a) Color map of the electric field strength. (b) Numerically calculated (solid curves) electric field strength E as a function of the distance r to the triangular wall edge in the direction y perpendicular to the wall for several angles β of the triangles. It is compared to the analytical result given by Eq. (13) and shown by dotted curves.

The comparison of analytical formula in Eq. (13) and the numerical result, shown in Fig. 3, indicates that Eq. (13) describes very well the electric field distribution near the edge. Therefore, to estimate the required electric field E_0 and voltage V_0 to hold ^4He film of thickness d_{He}^* near the wall edge we use Eqs. (8)-(13) with the upper cutoff equal to the period $l_R \sim 10 \mu\text{m}$ of the triangular grid. Eqs. (8),(12) and (13) give the required strength E_0 of the quasi-uniform electric field far from the wall edge:

$$E_0 \approx \frac{E^*}{\gamma} = \left(\frac{d_{\text{He}}^*}{l_R} \right)^{2\beta/(\pi+2\beta)} \lambda \sqrt{\frac{4\pi\rho_{\text{He}}gh}{\epsilon_{\text{He}} - 1}}. \quad (15)$$

For $d_{\text{He}}^* = 100 \text{ nm}$, $l_R \sim 10 \mu\text{m}$, and $\beta = \pi/4$, corresponding to straight edge angle $\alpha = \pi/2$, Eq. (15) gives $E_0 = 75 \text{ kV/cm}$. Taking $\alpha = \beta = \pi/3$ slightly reduces the required electric field intensity to $E_0 \approx 60 \text{ kV/cm}$.

The external electric field strength of $\sim 4 \text{ kV/cm}$ is rather common [50, 51] in the experiments with electrons on liquid

helium surface, but raising this electric field by an order of magnitude may be technically difficult. An electric field > 100 kV/cm was experimentally realized in a 1 cm gap between two electropolished stainless steel electrodes 12 cm in diameter for a wide range of pressures at $T = 0.4$ K [48]. The effect of a weaker electric field $E_0 \leq 45$ kV/cm on the superfluid helium scintillation produced by fast electrons or by α -particles at $T \geq 0.4$ K was also investigated experimentally [52, 53].

IV. EFFECT OF ELECTRIC FIELD ON RIPPLON DISPERSION

After solving the problem of coating the UCN trap walls by a sufficiently thick helium film, which protects UCN from the absorption inside the trap walls, the most important factor limiting the precision of UCN τ_n measurements is the inelastic neutron scattering by ripples – the quanta of surface waves. At low temperature $T < 0.5$ K, when the concentration of helium vapor is exponentially small, the main contribution to neutron scattering rate comes from low-frequency ripples with energy $\hbar\omega_q \sim V_0^{He} = 18.5$ neV [42]. The corresponding ripplon wave vector is still much larger than the inverse capillary length a_{He} of ^4He :

$$q_0 \approx \left[\left(V_0^{He} / \hbar \right)^2 \rho_{He} / \sigma_{He} \right]^{1/3} \approx 6.9 \mu\text{m}^{-1} \gg \kappa, \quad (16)$$

where $\kappa = a_{He}^{-1} = \sqrt{g\rho_{He}/\sigma_{He}} \approx 20 \text{ cm}^{-1}$. Hence, the ripplon dispersion at this wave vector is given by that of capillary waves: $\omega_q = \sqrt{\sigma_{He}/\rho_{He}} q^{3/2}$. If the electric field increases the ripplon energy $\hbar\omega_q$, this reduces the equilibrium ripplon density and the UCN scattering rate by ripples.

A. Uniform electric field

In a uniform electric field the ripplon dispersion law modifies [54] to

$$\omega_q^2 = gq + \frac{\sigma_{He}}{\rho_{He}} q^3 + \frac{(\varepsilon - 1)^2}{4\pi\rho_{He}\varepsilon(\varepsilon + 1)} \left(\varepsilon E_{||}^2 \cos^2 \theta - E_{\perp}^2 \right) q^2, \quad (17)$$

where $\varepsilon = \varepsilon_{He} = 1.054$ and the angle θ is between the electric field and the ripplon wave vector. For an electric field parallel to helium surface, as in Fig. 5, the field-induced correction to ripplon dispersion is positive and have a lower power of wave vector than the dominating capillary term. If this correction is large enough, it may reduce the UCN scattering rate by ripples. The ratio of the last electric term in Eq. (17), arising from ^4He polarization, to the second term, coming from capillary effect, for an electric field along the surface and parallel to q -vector, $E_{\perp} = 0$, and $\theta = 0$, is

$$\nu \equiv \frac{(\varepsilon - 1)^2 E_{||}^2}{4\pi(\varepsilon + 1)\sigma_{He}} \frac{1}{q_0} = \frac{(\varepsilon - 1)^2 e^2 E_{||}^2}{4\pi(\varepsilon + 1)\sigma_{He}} \frac{1}{e^2 q_0}. \quad (18)$$

Unfortunately, for ^4He in a reasonably strong external electric field $E_{||} = E_0 = 10$ kV/cm and at $q = q_0$ this ratio is too small:

$\nu \approx 5 \cdot 10^{-6}$. Even at $E_{||} = E_* = 230$ kV/cm this ratio at $q = q_0$ is not sufficient to change the ripplon dispersion considerably: $\nu(E_*) \approx 2.6 \cdot 10^{-3} \ll 1$. Hence, the correction to ripplon dispersion from a ^4He polarization in a uniform electric field, given by the last term in Eq. (17), is negligibly small and cannot help to reduce the UCN scattering rate by ripples.

B. Nonuniform electric field.

Eq. (17) is derived for a uniform electric field. A high nonuniform electric field, as on the surface of thin helium film near the edges of wall roughness, may change the ripplon dispersion stronger. According to Eq. (6), a nonuniform electric field creates a force

$$\mathbf{F} = -\nabla E_e = \frac{\varepsilon_{He} - 1}{4\pi} \int d^3\mathbf{r} \nabla [E^2(\mathbf{r})] \quad (19)$$

acting on ^4He volume. This force is added to the gravity force $F_g = \rho_{He}g \int d^3\mathbf{r}$ and renormalizes the free fall acceleration as

$$\mathbf{g} \rightarrow \mathbf{g}^*(\mathbf{r}) = \mathbf{g} - \frac{\varepsilon_{He} - 1}{4\pi\rho_{He}} \nabla [E^2(\mathbf{r})]. \quad (20)$$

For the triangular side-wall roughness near a sharp edge, $\beta \rightarrow \pi/2$, covered by ^4He film of thickness $d_{He}^* = 100$ nm we have

$$g^*(d_{He}^*) \sim \frac{\varepsilon_{He} - 1}{4\pi\rho_{He}} \frac{E_*^2}{d_{He}^*} \approx 1.75 \cdot 10^6 g. \quad (21)$$

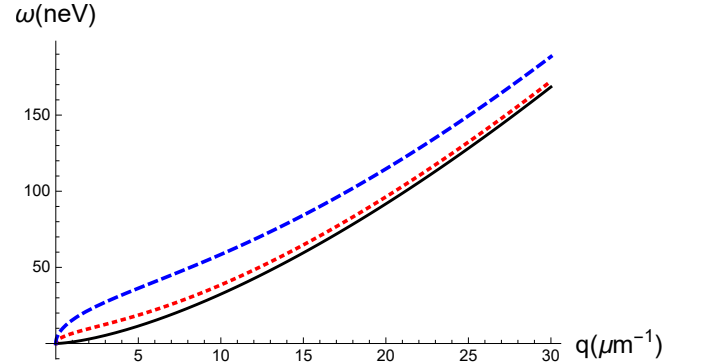


Figure 4. Ripplon dispersion, given by Eq. (23), for $g^*/g \approx 1$ (solid black line), $g^*/g \approx 10^7$ (dotted red line), and $g^*/g \approx 5.5 \cdot 10^7$ (dashed blue line).

To estimate the effect of nonuniform electric field near the wall edge covered by ^4He film at arbitrary β we substitute Eq. (12) to Eq. (20), which gives:

$$\frac{g^*(\mathbf{r})}{g} = 1 + \frac{\varepsilon_{He} - 1}{4\pi\rho_{He}g} \frac{4\beta\pi^2 E_0^2}{r(\pi + 2\beta)^3} \left(\frac{l}{r} \right)^{\frac{4\beta}{\pi + 2\beta}}. \quad (22)$$

For $r = d_{He}^* = 100$ nm, $l = l_R = 10$ μm , $E_0 = 60$ kV/cm, and $\beta = \pi/3$ this gives $g^*/g \approx 1.4 \cdot 10^6$. The corresponding $\kappa^* = \sqrt{g^*\rho_{He}/\sigma_{He}} \approx 2.4 \mu\text{m}^{-1} \sim q_0$. Hence, the ripplon dispersion

changes considerably at $q = q_0$ due to such a nonuniform electric field. Since at the trap bottom of UCN trap we do not need to hold liquid helium by a capillary effect, we may take a larger $l = l_R \sim 1$ mm. Then, according to Eq. (22) this raises g^*/g about $100^{4/5} \approx 40$ times to $g^*/g \approx 5.5 \cdot 10^7$. The corresponding ripplon dispersion, given by Eq. (17) without the last term but with renormalized g^* ,

$$\hbar\omega_q = \hbar\sqrt{g^*q + \frac{\sigma_{\text{He}}}{\rho_{\text{He}}}q^3}, \quad (23)$$

is shown in Fig. 4. It illustrates a considerable increase in ripplon energy $\hbar\omega_q$ at $q = q_0$. Hence, theoretically, a nonuniform electric field may reduce the UCN inelastic scattering rate by thermally activated ripplons. However, a more thorough calculation is needed to study this effect quantitatively at a nonuniform gradient of the electric field strength.

V. POSSIBLE TRAP DESIGNS

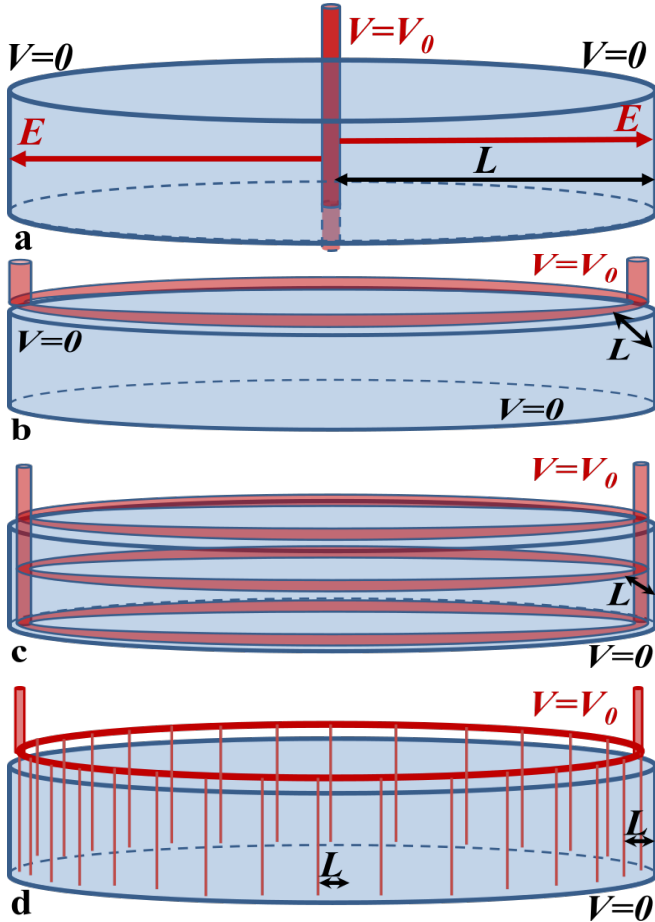


Figure 5. Possible UCN trap designs with electrostatic potential.

The voltage V_0 , corresponding to the required electric field E_0 and E_* , depends on the geometry of electrodes. In the trap design of Fig. 5a with the trap radius $L = R_{\text{trap}} = 1$ m

a strong field $E_0 \approx 60$ kV/cm requires a voltage difference $V_0 = E_0 L \approx 6$ MV, which is too high. In the trap design shown in Figs. 5b,c the electric field E_0 and voltage V_0 do not depend on the trap radius R_{trap} but only on the distance from the grounded side wall to the electrode at $V = V_0$.

The trap in Figs. 5b has only one toroidal electrode at $V = V_0$ placed at height $h_{\text{max}} = V_0^{\text{He}}/mng \approx 18$ cm above the helium level, i.e. just above the maximal height of UCN inside the trap. Then the distance $L \approx h_{\text{max}} - h$ depends on the height h on the wall from the helium level. At large height $h \sim h_{\text{max}}$, where the gravity energy to be compensated by electric field is the highest, the electric field $E_0(h) = V_0/L \approx V_0/(h_{\text{max}} - h)$ is also the highest. Then Eq. (15) gives

$$V_0 = \left(\frac{d_{\text{He}}}{l_R}\right)^{2\beta/(\pi+2\beta)} \lambda \sqrt{\frac{4\pi\rho_{\text{He}}gh}{\varepsilon_{\text{He}} - 1}} (h_{\text{max}} - h), \quad (24)$$

which has a maximal value

$$V_0^{\text{max}} = 0.385 \left(\frac{d_{\text{He}}}{l_R}\right)^{2\beta/(\pi+2\beta)} \lambda \sqrt{\frac{4\pi\rho_{\text{He}}gh_{\text{max}}^3}{\varepsilon_{\text{He}} - 1}}, \quad (25)$$

at $h = h_{\text{max}}/3 \approx 6$ cm. At this height one can take [44] $l_R = 4a_{\text{He}}^2/h \approx 17$ μm . Substituting this and $\alpha = \beta = \pi/3$ to Eq. (25) we obtain $V_0^{\text{max}} \approx 350$ kV $\approx E_0 h_{\text{max}}/3$, which is still very high and technically difficult. In Ref. [48] the realized voltage difference between two electrodes in ^4He was only $V_0 = 100$ kV.

The required voltage V_0 can be reduced by an order of magnitude or more if one uses the trap design shown in Fig. 5c with several toroidal electrodes at $V = V_0$ placed at different heights $h_i < h_{\text{max}}$ above the helium level. If these toroidal electrodes are rather thin and placed at a small distance $\sim l_R$ from the trap wall, theoretically, one can reduce the required voltage to only $V_0 \sim E_0 l_R \sim 60$ V. Technically, it may be more convenient to use the trap design illustrated in Fig. 5d, where thin wire electrodes hang down from the toroidal electrode above $h = h_{\text{max}}$.

An electrode at height $h < h_{\text{max}}$ may produce additional inelastic scattering of UCN inside the trap. This electrode is always covered by a helium film of thickness $d > 10$ nm due to the van-der-Waals forces, which attract helium vapor. However, for a safe protection of UCN by this ^4He film covering the electrodes we need $d \geq d_{\text{He}}^* = 100$ nm. Such a thick ^4He film can be held by either the surface roughness and capillary effect [43, 44], described by Eq. (5), or by the electrostatic energy of ^4He in electric field, given by Eq. (6). The latter is sufficient for a rather thin electrode. Indeed, the electric field around a cylindrical electrode of radius R_e is $E(r) \approx V_0/r/\ln(L/R_e) \approx E_0 L/r$. Hence, according to Eqs. (13) and (15), a commercially available copper wire of radius $R_e = 10$ μm [55] at voltage V_0 placed at a distance $L = 200$ $\mu\text{m} = 0.2$ mm from the grounded wall holds a ^4He film of sufficient thickness $d_{\text{He}}^* = 100$ nm $\ll R_e$ if

$$E(d_{\text{He}}^*) \approx \frac{V_0}{R_e \ln(L/R_e)} \geq E_* \approx 230 \text{ kV/cm},$$

or

$$V_0 \geq V_0^w = E_* R_e \ln(L/R_e). \quad (26)$$

For $R_e = 10 \mu\text{m}$ and $L = 0.5 \text{ mm}$ this gives $V_0 \geq 900 \text{ V}$. Thus, a sufficient ^4He coating of thin electrodes inside UCN trap is easy, because the voltage V_0 required for this coating is smaller than to hold ^4He film of sufficient thickness $d_{\text{He}}^* = 100 \text{ nm}$ on the side wall at height $h_{\text{max}} = 18 \text{ cm}$ above helium level. The latter at $\alpha = \beta = \pi/3$ requires $E_0 \approx 60 \text{ kV/cm}$, which for the $L = 0.2 \text{ mm}$ gives $V_0 \approx 1.2 \text{ kV}$. Hence, theoretically, by using the trap design in Figs. 5c,d one may reduce the required voltage to only $V_0 \sim 1 \text{ kV}$. Keeping two electrodes with voltage difference $V_0 \sim 1 \text{ kV}$ at a distance of only 0.2 mm remains technically difficult. One can increase the distance between electrodes at the cost of increasing their voltage difference. A smaller voltage holds a thinner ^4He film near the wall roughness edges, but it may still be useful to protect UCN from the absorption inside the trap walls.

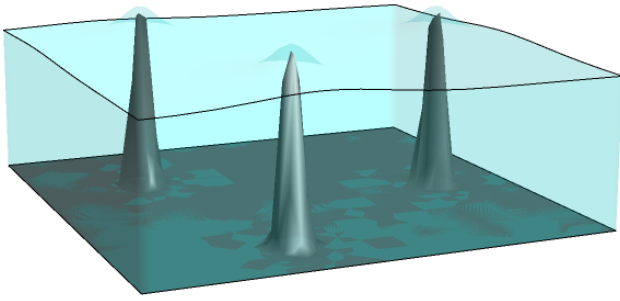


Figure 6. Schematic illustration of a 3D fur-like roughness of a metallic UCN trap wall holding a liquid helium film (light blue filling) by capillary effects. The applied electric field is the strongest near the wall peaks and holds additional amount of ^4He around these peaks, providing a complete coating of the UCN trap wall.

A 3D fur-like wall roughness with pyramidal or needle-shaped protrusions, as illustrated in Fig. 6, may further reduce the required voltage V_0 . The electric field at a distance r from a needle-like electrode at voltage U of curvature radius r_e above another electrode in the form of a plane perpendicular to the needle and separated by the distance L is [56]

$$E(r) \approx \frac{2U/\ln(4L/r_e)}{2r + r_e - r^2/L}. \quad (27)$$

Hence, in our case $L \gg l_R \gg r \sim d_{\text{He}}^* > r_e$ we have

$$E(r) \approx \frac{E_* d_{\text{He}}^*}{r + r_e/2} \approx \frac{E_0 l_R}{r + r_e/2}. \quad (28)$$

For $l_R \geq 5 \mu\text{m}$ and $r = d_{\text{He}}^* = 100 \text{ nm}$, the required electric field at the surface $E_* \approx 230 \text{ kV/cm}$ corresponds to the electric field $E_0 \lesssim 5 \text{ kV/cm}$ far from the edge. If the second electrode

is separated by a distance $L = 1 \text{ mm}$ from the wall, the required voltage is $V_0 = 500 \text{ V}$. However, making of such a wall with 3D fur-like roughness is more difficult than a cheap triangular diffraction grating, studied above.

VI. CONCLUSIONS

To summarize, we propose to improve the material UCN traps by coating with liquid helium using the combined effect of capillarity and of electric field. The side wall roughness holds a sufficiently thick ^4He film by the capillary effects [43, 44], but the very edges of this roughness remain coated by a too thin ^4He film. If this rough wall serves as an electrode, the electric field is the strongest near these wall edges, which attracts ^4He due to polarization forces. This helps to cover the wall edges and its entire surface by a sufficiently thick ^4He film to completely protect UCN from the absorption inside trap walls. The second electrode, if made in the form of thin wires, may be placed inside the UCN trap because it gets also coated by ^4He and does not absorb neutrons. The strong nonuniform electric field on the helium surface increases the ripplon energy, which makes their equilibrium concentration smaller. This reduces the inelastic scattering rate of UCN by riplons, but the effect is not sufficient to destroy this channel of UCN losses, which becomes dominating after the absorption of UCN inside trap walls is eliminated by their coating with liquid ^4He . Fortunately, the neutron-riplon interaction is weak, and the linear temperature dependence of UCN scattering rate by riplons helps to accurately take this systematic error into account [42]. A low temperature $T < 0.5 \text{ K}$ of trap walls is required to eliminate another source of UCN losses – scattering by helium vapor.

In spite of the mentioned technical difficulties, the proposed complete coating of UCN trap walls by liquid ^4He may give rise to a new generation of ultracold neutron traps with a very long storage time. This may strongly improve the precision of neutron lifetime measurements and of other experiments with ultracold neutrons.

VII. ACKNOWLEDGEMENTS

The work of P.D.G. is supported by the Russian Science Foundation grant # 23-22-00312. A.V.S. thanks the Foundation for the Advancement of Theoretical Physics and Mathematics "Basis" for grant # 22-1-1-24-1. V.D.K. acknowledges the financial support from the NUST "MISIS" grant No. K2-2022-025 in the framework of the federal academic leadership program Priority 2030. A.M.D. acknowledges the Ministry of Science and Higher Education of the Russian Federation (state assignment no. 0033-2019-0001 "Development of the Theory of Condensed Matter").

[1] H. Abele, Progress in Particle and Nuclear Physics **60**, 1 (2008), <https://www.sciencedirect.com/science/article/pii/S0146641007000622>.

[2] M. J. Ramsey-Musolf and S. Su, Physics Reports **456**, 1 (2008), <https://www.sciencedirect.com/science/article/pii/S0370157307003894>.

- [3] D. Dubbers and M. G. Schmidt, *Rev. Mod. Phys.* **83**, 1111 (2011), <https://link.aps.org/doi/10.1103/RevModPhys.83.1111>.
- [4] F. E. Wietfeldt and G. L. Greene, *Rev. Mod. Phys.* **83**, 1173 (2011), <https://link.aps.org/doi/10.1103/RevModPhys.83.1173>.
- [5] M. Gonzalez-Alonso, O. Naviliat-Cuncic, and N. Severijns, *Progress in Particle and Nuclear Physics* **104**, 165 (2019), <https://www.sciencedirect.com/science/article/pii/S0146641018300735>.
- [6] J. Liu, M. P. Mendenhall, A. T. Holley, H. O. Back, T. J. Bowles, L. J. Broussard, R. Carr, S. Clayton, S. Currie, B. W. Filippone, A. García, P. Geltenbort, K. P. Hickerson, J. Hoagland, G. E. Hogan, B. Hona, T. M. Ito, C.-Y. Liu, M. Makela, R. R. Mammei, J. W. Martin, D. Melconian, C. L. Morris, R. W. Pattie, A. Pérez Galván, M. L. Pitt, B. Plaster, J. C. Ramsey, R. Rios, R. Russell, A. Saunders, S. J. Seestrom, W. E. Sondheim, E. Tatar, R. B. Vogelaar, B. VornDick, C. Wrede, H. Yan, and A. R. Young (UCNA Collaboration), *Phys. Rev. Lett.* **105**, 181803 (2010), <https://link.aps.org/doi/10.1103/PhysRevLett.105.181803>.
- [7] B. Märkisch, H. Mest, H. Saul, X. Wang, H. Abele, D. Dubbers, M. Klopff, A. Petoukhov, C. Roick, T. Soldner, and D. Werder, *Phys. Rev. Lett.* **122**, 242501 (2019), <https://link.aps.org/doi/10.1103/PhysRevLett.122.242501>.
- [8] X. Sun, E. Adamek, B. Allgeier, Y. Bagdasarova, D. B. Berguno, M. Blatnik, T. J. Bowles, L. J. Broussard, M. A.-P. Brown, R. Carr, S. Clayton, C. Cude-Woods, S. Currie, E. B. Dees, X. Ding, B. W. Filippone, A. García, P. Geltenbort, S. Hasan, K. P. Hickerson, J. Hoagland, R. Hong, A. T. Holley, T. M. Ito, A. Knecht, C.-Y. Liu, J. Liu, M. Makela, R. Mammei, J. W. Martin, D. Melconian, M. P. Mendenhall, S. D. Moore, C. L. Morris, S. Nepal, N. Nouri, R. W. Pattie, A. Pérez Galván, D. G. Phillips, R. Picker, M. L. Pitt, B. Plaster, D. J. Salvat, A. Saunders, E. I. Sharapov, S. Sjue, S. Slutsky, W. Sondheim, C. Swank, E. Tatar, R. B. Vogelaar, B. VornDick, Z. Wang, W. Wei, J. W. Wexler, T. Womack, C. Wrede, A. R. Young, and B. A. Zeck (UCNA Collaboration), *Phys. Rev. C* **101**, 035503 (2020), <https://link.aps.org/doi/10.1103/PhysRevC.101.035503>.
- [9] M. Pospelov and A. Ritz, *Annals of Physics* **318**, 119 (2005), <https://www.sciencedirect.com/science/article/pii/S0003491605000539>.
- [10] C. A. Baker, D. D. Doyle, P. Geltenbort, K. Green, M. G. D. van der Grinten, P. G. Harris, P. Iaydjiev, S. N. Ivanov, D. J. R. May, J. M. Pendlebury, J. D. Richardson, D. Shiers, and K. F. Smith, *Phys. Rev. Lett.* **97**, 131801 (2006), <https://link.aps.org/doi/10.1103/PhysRevLett.97.131801>.
- [11] A. P. Serebrov, E. A. Kolomenskiy, A. N. Pirozhkov, I. A. Krasnoschekova, A. V. Vassiljev, A. O. Polushkin, M. S. Lasakov, A. K. Fomin, I. V. Shoka, V. A. Solovey, O. M. Zhrebtsov, P. Geltenbort, S. N. Ivanov, O. Zimmer, E. B. Alexandrov, S. P. Dmitriev, and N. A. Dovator, *JETP Letters* **99**, 4 (2014), <https://doi.org/10.1134/S0021364014010111>.
- [12] V. V. Nesvizhevsky, H. G. Börner, A. K. Petukhov, H. Abele, S. Baeßler, F. J. Rueß, T. Stöferle, A. Westphal, A. M. Gagarski, G. A. Petrov, and A. V. Strelkov, *Nature* **415**, 297 (2002), <https://doi.org/10.1038/415297a>.
- [13] T. Jenke, G. Cronenberg, J. Burgdörfer, L. A. Chizhova, P. Geltenbort, A. N. Ivanov, T. Lauer, T. Lins, S. Rother, H. Saul, U. Schmidt, and H. Abele, *Phys. Rev. Lett.* **112**, 151105 (2014), <https://link.aps.org/doi/10.1103/PhysRevLett.112.151105>.
- [14] R. Golub, D. Richardson, and L. S. K., *Ultra-Cold Neutrons* (CRC Press, 1991) <https://doi.org/10.1201/9780203734803>.
- [15] V. K. Ignatovich, *The Physics of Ultracold Neutrons* (Clarendon Press, 1990) <https://isbsearch.org/isbn/0198510152>.
- [16] V. K. Ignatovich, *Physics-Uspekhi* **39**, 283 (1996), <https://doi.org/10.1070/pu1996v039n03abeh000138>.
- [17] A. P. Serebrov, V. E. Varlamov, A. G. Kharitonov, A. K. Fomin, Y. N. Pokotilovski, P. Geltenbort, I. A. Krasnoschekova, M. S. Lasakov, R. R. Taldaev, A. V. Vassiljev, and O. M. Zhrebtsov, *Phys. Rev. C* **78**, 035505 (2008), <https://link.aps.org/doi/10.1103/PhysRevC.78.035505>.
- [18] S. Arzumanov, L. Bondarenko, S. Chernyavsky, P. Geltenbort, V. Morozov, V. V. Nesvizhevsky, Y. Panin, and A. Strepotov, *Physics Letters B* **745**, 79 (2015), <https://www.sciencedirect.com/science/article/pii/S0370269315002646>.
- [19] A. P. Serebrov, E. A. Kolomenskiy, A. K. Fomin, I. A. Krasnoschekova, A. V. Vassiljev, D. M. Prudnikov, I. V. Shoka, A. V. Chechkin, M. E. Chaikovskii, V. E. Varlamov, S. N. Ivanov, A. N. Pirozhkov, P. Geltenbort, O. Zimmer, T. Jenke, M. Van der Grinten, and M. Tucker, *JETP Letters* **106**, 623 (2017), <https://doi.org/10.1134/S0021364017220143>.
- [20] A. P. Serebrov, E. A. Kolomenskiy, A. K. Fomin, I. A. Krasnoschekova, A. V. Vassiljev, D. M. Prudnikov, I. V. Shoka, A. V. Chechkin, M. E. Chaikovskii, V. E. Varlamov, S. N. Ivanov, A. N. Pirozhkov, P. Geltenbort, O. Zimmer, T. Jenke, M. Van der Grinten, and M. Tucker, *Phys. Rev. C* **97**, 055503 (2018), <https://link.aps.org/doi/10.1103/PhysRevC.97.055503>.
- [21] Pattie, R. W., Callahan, N. B., Cude-Woods, C., Adamek, E. R., Adams, M., Barlow, D., Blatnik, M., D., Bowman, Broussard, L. J., Clayton, S., Currie, S., Dees, E. B., Ding, X., Fellers, D., Fox, W., Fries, E., Gonzalez, F., Geltenbort, P., Hickerson, K. P., Hoffbauer, M. A., Hoffman, K., Holley, A. T., Howard, D., Ito, T. M., Komives, A., Liu, C. Y., M., Makela, Medina, J., Morley, D., Morris, C. L., O'Connor, T., Penttilä, S.I., Ramsey, J.C., Roberts, A., Salvat, D., Saunders, A., Seestrom, S.J., Sharapov, E.I., Sjue, S.K.L., Snow, W.M., Sprow, A., Vanderwerp, J., Vogelaar, B., P.L., Walstrom, Wang, Z., Weaver, H., Wexler, J., Womack, T.L., Young, A.R., and Zeck, B.A., *EPJ Web Conf.* **219**, 03004 (2019), <https://doi.org/10.1051/epjconf/201921903004>.
- [22] W. Mampe, P. Ageron, C. Bates, J. M. Pendlebury, and A. Steyerl, *Phys. Rev. Lett.* **63**, 593 (1989), <https://link.aps.org/doi/10.1103/PhysRevLett.63.593>.
- [23] A. Pichlmaier, V. Varlamov, K. Schreckenbach, and P. Geltenbort, *Physics Letters B* **693**, 221 (2010), <https://www.sciencedirect.com/science/article/pii/S0370269310009792>.
- [24] P. R. Huffman, C. R. Brome, J. S. Butterworth, K. J. Coakley, M. S. Dewey, S. N. Dzhosyuk, R. Golub, G. L. Greene, K. Habicht, S. K. Lamoreaux, C. E. H. Mattoni, D. N. McKinsey, F. E. Wietfeldt, and J. M. Doyle, *Nature* **403**, 62 (2000), <https://doi.org/10.1038/47444>.
- [25] K. K. H. Leung, P. Geltenbort, S. Ivanov, F. Rosenau, and O. Zimmer, *Phys. Rev. C* **94**, 045502 (2016), <https://link.aps.org/doi/10.1103/PhysRevC.94.045502>.
- [26] A. Steyerl, K. K. H. Leung, C. Kaufman, G. Müller, and S. S. Malik, *Phys. Rev. C* **95**, 035502 (2017), <https://link.aps.org/doi/10.1103/PhysRevC.95.035502>.
- [27] V. F. Ezhov, A. Z. Andreev, G. Ban, B. A. Bazarov, P. Geltenbort, A. G. Glushkov, V. A. Knyazkov, N. A. Kovrizhnykh, G. B. Krygin, O. Naviliat-Cuncic, and V. L. Ryabov, *JETP Letters* **107**, 671 (2018), <https://doi.org/10.1134/S0021364018110024>.

- [28] R. W. Pattie, N. B. Callahan, C. Cude-Woods, E. R. Adamek, L. J. Broussard, S. M. Clayton, S. A. Currie, E. B. Dees, X. Ding, E. M. Engel, D. E. Fellers, W. Fox, P. Geltenbort, K. P. Hickerson, M. A. Hoffbauer, A. T. Holley, A. Komives, C.-Y. Liu, S. W. T. MacDonald, M. Makela, C. L. Morris, J. D. Ortiz, J. Ramsey, D. J. Salvat, A. Saunders, S. J. Seestrom, E. I. Sharapov, S. K. Sjue, Z. Tang, J. Vanderwerp, B. Vogelaar, P. L. Walstrom, Z. Wang, W. Wei, H. L. Weaver, J. W. Wexler, T. L. Womack, A. R. Young, and B. A. Zeck, *Science* **360**, 627 (2018), <https://science.sciencemag.org/content/360/6389/627>, <https://science.sciencemag.org/content/360/6389/627.full.pdf>.
- [29] J. S. Nico, M. S. Dewey, D. M. Gilliam, F. E. Wietfeldt, X. Fei, W. M. Snow, G. L. Greene, J. Pauwels, R. Eykens, A. Lamberty, J. V. Gestel, and R. D. Scott, *Phys. Rev. C* **71**, 055502 (2005), <https://link.aps.org/doi/10.1103/PhysRevC.71.055502>.
- [30] A. T. Yue, M. S. Dewey, D. M. Gilliam, G. L. Greene, A. B. Laptev, J. S. Nico, W. M. Snow, and F. E. Wietfeldt, *Phys. Rev. Lett.* **111**, 222501 (2013), <https://link.aps.org/doi/10.1103/PhysRevLett.111.222501>.
- [31] K. Hirota, G. Ichikawa, S. Ieki, T. Ino, Y. Iwashita, M. Kitaguchi, R. Kitahara, J. Koga, K. Mishima, T. Mogi, K. Morikawa, A. Morishita, N. Nagakura, H. Oide, H. Okabe, H. Otono, Y. Seki, D. Sekiba, T. Shima, H. M. Shimizu, N. Sumi, H. Sumino, T. Tomita, H. Uehara, T. Yamada, S. Yamashita, K. Yano, M. Yokohashi, and T. Yoshioka, *Progress of Theoretical and Experimental Physics* **2020**, 10.1093/ptep/ptaa169 (2020), <https://doi.org/10.1093/ptep/ptaa169>, <https://academic.oup.com/ptep/article-pdf/2020/12/123C02/35931162/ptaa169.pdf>.
- [32] S. Rajendran and H. Ramani, *Phys. Rev. D* **103**, 035014 (2021), <https://link.aps.org/doi/10.1103/PhysRevD.103.035014>.
- [33] A. P. Serebrov, M. E. Chaikovskii, G. N. Klyushnikov, O. M. Zherebtsov, and A. V. Chechkin, *Phys. Rev. D* **103**, 074010 (2021), <https://link.aps.org/doi/10.1103/PhysRevD.103.074010>.
- [34] A. P. Serebrov, *Physics-Uspekhi* **62**, 596 (2019).
- [35] D. Dubbers, H. Saul, B. Märkisch, T. Soldner, and H. Abele, *Physics Letters B* **791**, 6 (2019).
- [36] E. A. Goremychkin and Y. N. Pokotilovski, *JETP Letters* **105**, 548 (2017).
- [37] R. Golub, C. Jewell, P. Ageron, W. Mampe, B. Heckel, and I. Kilvington, *Zeitschrift für Physik B Condensed Matter* **51**, 187 (1983).
- [38] R. C. Bokun, *Sov. J. Nucl. Phys.* **40**, 287 (1984), <https://inis.iaea.org/search/searchsingle.asp?recordsFor=SingleRecord&RN=16073419>.
- [39] V. P. Alfimenkov, V. K. Ignatovich, L. P. Mezhev-Deglin, V. I. Morozov, A. V. Strelkov, and T. M. I., *Communications of Joint Institute for Nuclear Research, Dubna preprint (in Russian)* **P3-2009-197** (2009), [http://www1.jinr.ru/Preprints/2009/197\(P3-2009-197\).pdf](http://www1.jinr.ru/Preprints/2009/197(P3-2009-197).pdf).
- [40] S. Ahmed, E. Altieri, T. Andalib, B. Bell, C. P. Bidinosti, E. Cudmore, M. Das, C. A. Davis, B. Franke, M. Gericke, P. Giampa, P. Gnyp, S. Hansen-Romu, K. Hatanaka, T. Hayamizu, B. Jamieson, D. Jones, S. Kawasaki, T. Kikawa, M. Kitaguchi, W. Klassen, A. Konaka, E. Korkmaz, F. Kuchler, M. Lang, L. Lee, T. Lindner, K. W. Madison, Y. Makida, J. Mammei, R. Mammei, J. W. Martin, R. Matsumiya, E. Miller, K. Mishima, T. Momose, T. Okamura, S. Page, R. Picker, E. Pierre, W. D. Ramsay, L. Rebenitsch, F. Rehm, W. Schreyer, H. M. Shimizu, S. Sidhu, A. Sikora, J. Smith, I. Tanihata, B. Thorsteinson, S. Vanbergen, W. T. H. van Oers, and Y. X. Watanabe (TUCAN Collaboration), *Phys. Rev. C* **99**, 025503 (2019), <https://link.aps.org/doi/10.1103/PhysRevC.99.025503>.
- [41] O. Zimmer, *Phys. Rev. C* **93**, 035503 (2016), <https://link.aps.org/doi/10.1103/PhysRevC.93.035503>.
- [42] P. D. Grigoriev, O. Zimmer, A. D. Grigoriev, and T. Ziman, *Phys. Rev. C* **94**, 025504 (2016), <https://link.aps.org/doi/10.1103/PhysRevC.94.025504>.
- [43] P. D. Grigoriev and A. M. Dyugaev, *Phys. Rev. C* **104**, 055501 (2021).
- [44] P. D. Grigoriev, A. M. Dyugaev, T. I. Mogilyuk, and A. D. Grigoriev, *JETP Letters* **114**, 493 (2021).
- [45] Diffraction gratings with the period $l_R = 1 \mu\text{m}$ and dimensions $1.524 \times 0.1524\text{m}$ are available at a price of \$20 at www.amazon.com.
- [46] G. V. Kulin, A. I. Frank, S. V. Goryunov, P. Geltenbort, M. Jentschel, V. A. Bushuev, B. Lauss, P. Schmidt-Wellenburg, A. Panzarella, and Y. Fuchs, *Phys. Rev. A* **93**, 033606 (2016).
- [47] G. Kulin, A. Frank, M. Zakharov, S. Goryunov, V. Bushuev, A. Panzarella, P. Geltenbort, and M. Jentschel, *Journal of Experimental and Theoretical Physics* **129**, 806 (2019).
- [48] T. M. Ito, J. C. Ramsey, W. Yao, D. H. Beck, V. Cianciolo, S. M. Clayton, C. Crawford, S. A. Currie, B. W. Filippone, W. C. Griffith, M. Makela, R. Schmid, G. M. Seidel, Z. Tang, D. Wagner, W. Wei, and S. E. Williamson, *Review of Scientific Instruments* **87**, 045113 (2016), <https://doi.org/10.1063/1.4946896>.
- [49] K. Binns and P. Lawrenson, *Analysis and Computation of Electric and Magnetic Field Problems*, Pergamon international library of science, technology, engineering, and social studies (Elsevier Science & Technology, 1973).
- [50] A. P. Volodin, M. S. Khaikin, and V. S. Edelman, *JETP Letters* **26**, 543 (1977).
- [51] P. Leiderer, *Journal of Low Temperature Physics* **87**, 247 (1992).
- [52] T. M. Ito, S. M. Clayton, J. Ramsey, M. Karcz, C.-Y. Liu, J. C. Long, T. G. Reddy, and G. M. Seidel, *Phys. Rev. A* **85**, 042718 (2012).
- [53] N. S. Phan, V. Cianciolo, S. M. Clayton, S. A. Currie, R. Dipert, T. M. Ito, S. W. T. MacDonald, C. M. O'Shaughnessy, J. C. Ramsey, G. M. Seidel, E. Smith, E. Tang, Z. Tang, and W. Yao, *Phys. Rev. C* **102**, 035503 (2020).
- [54] L. A. Mel'nikovskii and S. A. Kriminskii, *Journal of Experimental and Theoretical Physics* **84**, 758 (1997).
- [55] Bobbins with ultra thin copper wires of diameter $10 \mu\text{m}$ are available for \$10.99 at www.amazon.com.
- [56] B. Florkowska and R. Wlodek, *IEEE Transactions on Electrical Insulation* **28**, 932 (1993).